

# ChemComm

Accepted Manuscript



This is an *Accepted Manuscript*, which has been through the Royal Society of Chemistry peer review process and has been accepted for publication.

*Accepted Manuscripts* are published online shortly after acceptance, before technical editing, formatting and proof reading. Using this free service, authors can make their results available to the community, in citable form, before we publish the edited article. We will replace this *Accepted Manuscript* with the edited and formatted *Advance Article* as soon as it is available.

You can find more information about *Accepted Manuscripts* in the [Information for Authors](#).

Please note that technical editing may introduce minor changes to the text and/or graphics, which may alter content. The journal's standard [Terms & Conditions](#) and the [Ethical guidelines](#) still apply. In no event shall the Royal Society of Chemistry be held responsible for any errors or omissions in this *Accepted Manuscript* or any consequences arising from the use of any information it contains.

## COMMUNICATION

# A Fundamental Study on the $[(\mu\text{-Cl})_3\text{Mg}_2(\text{THF})_6]^+$ Dimer Electrolytes for Rechargeable Mg Batteries

Cite this: DOI: 10.1039/x0xx00000x

Tianbiao Liu,<sup>\*a</sup> Jonathan T. Cox,<sup>b</sup> Dehong Hu,<sup>c</sup> Xuchu Deng,<sup>c</sup> Jianzhi Hu,<sup>c</sup> Mary Y. Hu,<sup>c</sup> Jie Xiao, Yuyan Shao,<sup>a</sup> Keqi Tang,<sup>b</sup> and Jun Liu<sup>\*a</sup>

Received 00th January 2012,

Accepted 00th January 2012

DOI: 10.1039/x0xx00000x

www.rsc.org/

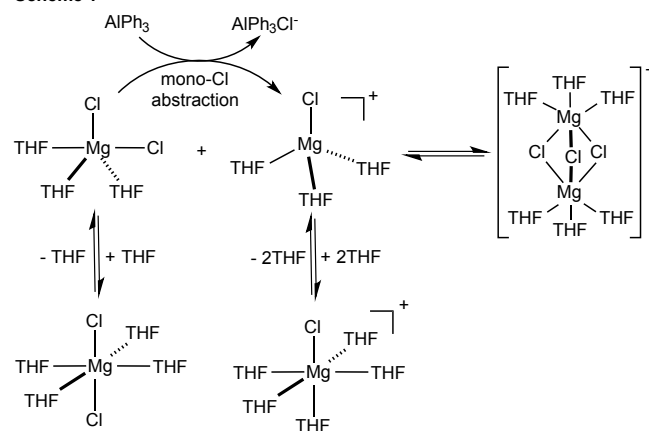
**Long sought  $[\text{MgCl}]^+$  solution species in the Mg-dimer electrolytes was characterized by a soft mass spectrometry. The presented study provides insightful understandings on the electrolyte chemistry of rechargeable Mg batteries.**

To address the global problems of escalating energy demand and increasing emissions of  $\text{CO}_2$ , it is critical to develop effective approaches to convert renewable but intermittently available energy sources (e.g. solar and wind energy) into reliable energy forms. Battery systems with low cost, high energy density and long cycling life time have been suggested as viable technologies for storing sustainable energy.<sup>1</sup> Recently rechargeable Magnesium (Mg) batteries have been advocated as promising battery systems alternative to lithium or sodium based batteries for grid scale energy storage, powering portable devices, and transportation applications.<sup>1a, 2</sup> There are several technic advantages of Mg batteries over Li batteries and Na batteries. Mg is earth abundant and low cost (ca. 24 times cheaper than Li). As an anode material, Mg is safe to use without dendrite formation (vs Li, Li-ion or Na batteries) and high volumetric capacity (3832 Ah/L vs 2062 Ah/L for Li and 1165 Ah/L for Na) due to its two-electron redox chemistry. Mg based electrolytes are environmentally benign. Furthermore, Mg has a sufficient high reduction potential (-2.37 V vs SHE) amenable for assembling high energy density batteries with suitable cathode materials.

In 1990, Gregory *et al.* made a major breakthrough on electrochemical Mg deposition by using Al or B Lewis acid additives to enhance electrochemical performance of Grignard reagents and  $\text{MgBu}_2$  electrolytes.<sup>3</sup> Since then, there have been continuous efforts in developing Mg conductive electrolytes for rechargeable Mg batteries by Aurbach<sup>4</sup> and others.<sup>5</sup> We have put our efforts in developing advanced Mg electrolytes with improved oxidation stability and electrophile compatibility by avoiding the use of nucleophilic Mg sources such as Grignard reagents or dialkyl magnesium.<sup>6</sup> Poor oxidation stability and/or undesired nucleophilicity of the reported electrolytes prepared from nucleophilic Mg sources are attributed to reactive alkyl or aryl anions in these reagents.<sup>4b, 6</sup> Based on a straightforward retrosynthesis analysis on the  $[(\mu\text{-Cl})_3\text{Mg}_2(\text{THF})_6]^+$  dimer, a common recrystallized product of popular Mg-Cl complex electrolytes,<sup>4b, 5a, 5c, 7</sup> we developed a facile approach (termed as *mono-Cl abstraction*,

see Scheme 1) using  $\text{MgCl}_2$  and an Al Lewis acid to produce high performance Mg-dimer containing electrolytes.<sup>6</sup>

Scheme 1



The  $\text{MgCl}_2$ -Al Lewis acid electrolytes are much cleaner compared to electrolytes made from nucleophilic Mg reagents in terms of composition because of the simply and clean  $\text{Cl}^-$  metathesis reaction without complication by nucleophilic alkyl or aryl species.<sup>5c, 6</sup> Therefore, these electrolytes provide a unique opportunity to understand solution chemistry of the  $[(\mu\text{-Cl})_3\text{Mg}_2(\text{THF})_6]^+$  dimer and further its electrochemical behaviors. Previously, we proposed a reaction mechanism for the formation of the Mg-dimer coordination complex from  $\text{MgCl}_2$  and an Al Lewis acid in the mono-Cl approach (see Scheme 1). THF solvated  $\text{MgCl}_2$ , *trans*- $\text{MgCl}_2(\text{THF})_4$ , undergoes THF dissociation and subsequent mono-Cl abstraction by an Al Lewis acid (e.g.  $\text{AlPh}_3$  in Scheme 1) to generate the reactive intermediate  $[\text{MgCl}]^+$  cation,  $[\text{MgCl}(\text{THF})_3]^+$ . Coordination unsaturation of  $[\text{MgCl}(\text{THF})_3]^+$  can promote a dimerization reaction with  $\text{MgCl}_2(\text{THF})_3$  to result in the Mg-dimer cation.<sup>4b, 6</sup> Both  $[(\mu\text{-Cl})_3\text{Mg}_2(\text{THF})_6]^+$ <sup>5c</sup> and  $[\text{MgCl}(\text{THF})_5]^+$ <sup>2b</sup> have been proposed to be the active species responsible for electrochemical Mg cycling. However, there is no experimental evidence for the existence of THF solvated  $[\text{MgCl}]^+$  in the solution of dimer electrolytes.<sup>4b</sup> In this study, we report the first experimental evidence of a solution  $[\text{MgCl}]^+$  species,  $[\text{MgCl}(\text{THF})_3]^+$ , in Mg dimer electrolytes using SPIN (Subambient Pressure Ionization with Nanoelectrospray) mass spectrometry.<sup>8</sup> In

combination with additional results, the coordination chemistry of the Mg-dimer electrolytes is elucidated and electrochemical mechanisms involving  $\text{Mg}^{2+}$  and  $\text{Cl}^-$  transports for reversible Mg deposition and stripping of the Mg dimer electrolytes are proposed and discussed.

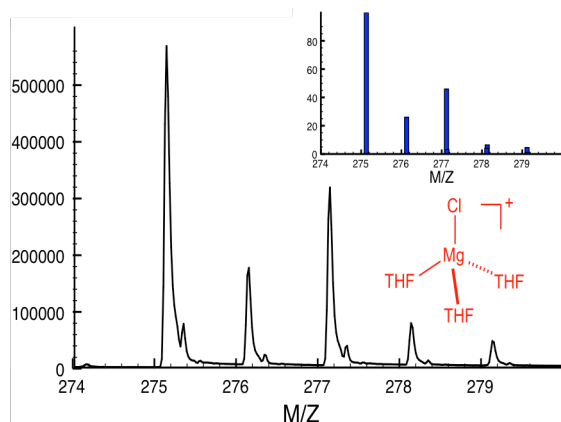


Figure 1. The M/Z isotopic distribution of the  $[\text{MgCl}(\text{THF})_3]^+$  peak in the positive mode of SPIN MS of  $[(\mu\text{-Cl})_3\text{Mg}_2(\text{THF})_6]\text{AlPh}_3\text{Cl}$ . Inset gives the calculated isotopic pattern for  $[\text{MgCl}(\text{THF})_3]^+$ .

In an effort to further understand the chemical nature of the Mg dimer electrolytes and elucidate the proposed reaction mechanism,<sup>4b, 6</sup> we have attempted to detect the  $[\text{MgCl}]^+$  mono-cation in our electrolyte solution. We first tried conventional electrospray ionization (ESI) MS as the technique can resolve charged species through values of mass charge ratio (M/Z) and corresponding isotopic patterns. However, there was no meaningful species detected in the positive mode of ESI-MS with  $[(\mu\text{-Cl})_3\text{Mg}_2(\text{THF})_6]\text{AlPh}_3\text{Cl}$  at different concentrations (from 0.05 mM up to 5 mM). Similar results were obtained with  $[(\mu\text{-Cl})_3\text{Mg}_2(\text{THF})_6]\text{AlCl}_4$  and  $[(\mu\text{-Cl})_3\text{Mg}_2(\text{THF})_6]\text{AlEtCl}_3$  electrolytes.<sup>6</sup> We rationalized Mg-THF coordination interaction is too labile to survive under typical ESI-MS interface configuration which operates with an inlet temperature of 200 °C. So we started to seek a MS technique with a softer ESI source. We found out Subambient Pressure Ionization with Nano-electrospray Mass spectrometry (SPIN-MS)<sup>8</sup> is a unique MS interface technique with high ionization efficiency and a softer ion source to enable the characterization of compounds with weak chemical bonds with high sensitivity. The SPIN source can be operated at a temperature below 80 °C and may provide a chance to detect positively charged THF solvated  $[\text{MgCl}]^+$  species. To our delight, a  $[\text{MgCl}]^+$  species with three THF coordinated,  $[\text{MgCl}(\text{THF})_3]^+$ , was consistently identified at 275.13 M/Z by SPIN-MS (Figure 1) for  $[(\mu\text{-Cl})_3\text{Mg}_2(\text{THF})_6]\text{AlPh}_3\text{Cl}$  THF solution. The match of the experimental and calculated isotope patterns further confirms its identity (Figure 1).  $[\text{MgCl}(\text{THF})_3]^+$  is either directly from the solution or generated from  $[\text{MgCl}(\text{THF})_5]^+$  during the ionization process. In the later case, the result suggests Mg-THF bonds in  $[\text{MgCl}(\text{THF})_3]^+$  is stronger than the ones in  $[\text{MgCl}(\text{THF})_5]^+$ . However, no signal was observed for the dimer cation. Preliminary DFT calculations suggest the  $[\text{MgCl}]^+$  monomer is more dominant over the dimer cation in the equilibrium, which explains a lower possibility to observe the dimer cation. A recent study also suggests the dimer is preferred in solid state.<sup>9</sup> Another possibility is the lack of sufficient stability of the dimer cation under the testing conditions. Consistently, the  $[\text{MgCl}(\text{THF})_3]^+$  cation was also clearly identified in the  $[(\mu\text{-Cl})_3\text{Mg}_2(\text{THF})_6]\text{AlEtCl}_3$  electrolyte (Figure S4). The SPIN-MS studies of the  $\text{MgCl}_2$  THF solution without adding an Al Lewis acid did not show the monocation signal.

To the best of our knowledge, the SPIN MS result is the first experimental evidence for the existence of THF solvated  $[\text{MgCl}]^+$  mono-cation in the solution of  $[(\mu\text{-Cl})_3\text{Mg}_2(\text{THF})_6]^+$  dimer electrolytes. The identification of the  $[\text{MgCl}(\text{THF})_3]^+$  mono-cation establishes the reaction nature of mono-Cl abstraction of solvated  $\text{MgCl}_2$  by an Al Lewis acid as described above (see Scheme 1).

Raman spectroscopic studies of  $[(\mu\text{-Cl})_3\text{Mg}_2(\text{THF})_6]\text{AlPh}_3\text{Cl}$  in solution were first attempted but no resolved spectrum was obtained due to strong fluorescence. The Raman spectrum of  $[(\mu\text{-Cl})_3\text{Mg}_2(\text{THF})_6]\text{AlPh}_3\text{Cl}$  in solid state confirmed the presence of the solvated  $\text{MgCl}_2$  species, showing a diagnostic peak at 209  $\text{cm}^{-1}$  (Figure 2). The weak peak at 252  $\text{cm}^{-1}$  is assigned to  $[(\mu\text{-Cl})_3\text{Mg}_2(\text{THF})_6]^+$  and two peaks at 618 and 653  $\text{cm}^{-1}$  are attributed to phenyl ligand ring wagging of the  $\text{AlPh}_3\text{Cl}^-$  anion.<sup>4b</sup> The SPIN Mass, Raman spectroscopic results, and the established solid structure of  $[(\mu\text{-Cl})_3\text{Mg}_2(\text{THF})_6]\text{AlPh}_3\text{Cl}$ ,<sup>6</sup> provide a full experimental picture on the equilibrium between  $[(\mu\text{-Cl})_3\text{Mg}_2(\text{THF})_6]^+$  and THF solvated  $[\text{MgCl}]^+$  and  $\text{MgCl}_2$ .

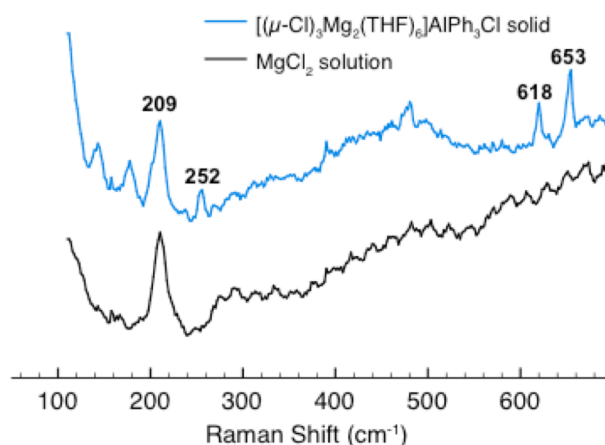


Figure 2. Raman Spectra of solid  $[(\mu\text{-Cl})_3\text{Mg}_2(\text{THF})_6]\text{AlPh}_3\text{Cl}$  (blue trace) and  $\text{MgCl}_2$  THF solution (black trace).

$\text{Cl}^-$  is the primary ligand in supporting the coordination structures of solution  $\text{Mg}^{2+}$  species and defines their electronic structures, i.e. frontier HOMO and LUMO energy that are closely associated with redox potentials of electron transfer reactions. Studying  $\text{Cl}^-$  ligand behaviors could lead to further insights into the  $[(\mu\text{-Cl})_3\text{Mg}_2(\text{THF})_6]^+$  dimer and its equilibrumers in terms of  $\text{Cl}^-$  and  $\text{Mg}^{2+}$  ion transports, and electrochemical Mg deposition and stripping. Aurbach *et al.* reported external  $\text{Cl}^-$  anion can affect the chemical equilibrium of  $[(\mu\text{-Cl})_3\text{Mg}_2(\text{THF})_6]^+$  and suggested  $[\text{MgCl}_4]^{2-}$  species is formed in the reaction of the APC electrolyte with  $\text{Cl}^-$ .<sup>10</sup> However, the presence of  $\text{MgPh}_2$  in the APC electrolyte<sup>6</sup> can also react with external  $\text{Cl}^-$  due to the Schlenk equilibrium and complicate data interpretation. As our electrolytes are less complex than Aurbach's all phenyl complex (APC) electrolytes,<sup>4b, 6, 10</sup> we anticipate our electrolytes would provide new insights into the reactivities of the  $[(\mu\text{-Cl})_3\text{Mg}_2(\text{THF})_6]^+$  dimer electrolyte with  $\text{Cl}^-$ . So we have investigated the  $\text{Cl}^-$  effect on the  $[(\mu\text{-Cl})_3\text{Mg}_2(\text{THF})_6]\text{AlPh}_3\text{Cl}$  electrolyte using various physical methods.

<sup>25</sup> $\text{Mg}\{^1\text{H}\}$  NMR studies were carried out to monitor the effect of  $\text{Cl}^-$  on the <sup>25</sup>Mg chemical shift of  $[(\mu\text{-Cl})_3\text{Mg}_2(\text{THF})_6]^+$ . As shown in Figure 3,  $[(\mu\text{-Cl})_3\text{Mg}_2(\text{THF})_6]\text{AlPh}_3\text{Cl}$  exhibits a broad singlet at 5.3 ppm, consistent with an exchange process of the dimer with solvated  $[\text{MgCl}_2]$  and  $[\text{MgCl}]^+$  species. With addition of tetrabutylammonium chloride (TBACl) as the  $\text{Cl}^-$  source, the Mg resonance gradually shifts from 5.3 ppm to lower field up to 11.9

ppm at 0.1 M Cl<sup>-</sup> (Figure 3 and Figure S1). In the same time, the peak width of the Mg resonances broadens from 207.5 Hz to 419 Hz (see Figure S1), indicating a slower exchange process with increasing Cl<sup>-</sup> concentration. The changes of the chemical shift and its peak width are consistent with formation of new Mg species or a change of the chemical equilibrium of  $[(\mu\text{-Cl})_3\text{Mg}_2(\text{THF})_6]^+$  upon addition of Cl<sup>-</sup>. During the addition of Cl<sup>-</sup>, there was no precipitate of MgCl<sub>2</sub> formed. The solution after adding Cl<sup>-</sup> stayed in clear for days. No obvious spectroscopic change was observed in the <sup>27</sup>Al{<sup>1</sup>H} NMR spectrum after addition of Cl<sup>-</sup> (Figure S2). To gain further understandings of the chemical equilibrium, the solution of 1:1 ratio of  $[(\mu\text{-Cl})_3\text{Mg}_2(\text{THF})_6]\text{AlPh}_3\text{Cl}$  and TBACl was examined by SPIN MS. It was found out the signal of  $[\text{MgCl}(\text{THF})_3]^+$  at 275.2 M/Z became significantly more intensive than the sample of  $[(\mu\text{-Cl})_3\text{Mg}_2(\text{THF})_6]\text{AlPh}_3\text{Cl}$  without adding Cl<sup>-</sup> (Figure S3). However, attempted SPIN-MS negative mode experiments did not identify new Mg species, either of  $[\text{MgCl}_3(\text{THF})]^-$  or  $[\text{MgCl}_4]^{2-}$ .

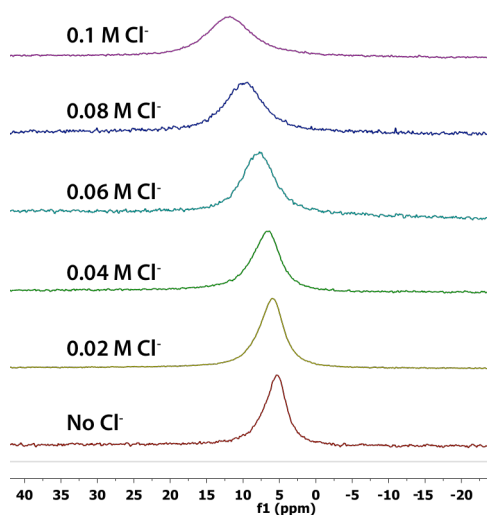


Figure 3. <sup>25</sup>Mg NMR spectra of  $[(\mu\text{-Cl})_3\text{Mg}_2(\text{THF})_6]\text{AlPh}_3\text{Cl}$ , 0.1 M in THF (collected at 25 °C) in the presence of tetrabutylammonium chloride (TBACl) at different concentrations as indicated.

Figure 4 displays the cyclic voltammograms of  $[(\mu\text{-Cl})_3\text{Mg}_2(\text{THF})_6]\text{AlPh}_3\text{Cl}$  at various concentrations of TBACl. With increasing Cl<sup>-</sup> concentration to 0.02 M, the current intensities of Mg deposition and stripping initially increased, consistent with enhanced solution conductivity (Figure S6). However, when Cl<sup>-</sup> concentration is above 0.03 M, the current start to decrease. To clearly demonstrate the experimental observation, a plot of Mg deposition and stripping charge versus Cl<sup>-</sup> concentration is given in Figure S6. In the meanwhile, solution conductivity (0.96 mS/cm at 0.02 M Cl<sup>-</sup>) started to decrease while there is not an apparent relationship between solution conductivity and Cl<sup>-</sup> concentration (Figure S6). The effect of Cl<sup>-</sup> on the electrochemical behaviors of  $[(\mu\text{-Cl})_3\text{Mg}_2(\text{THF})_6]\text{AlPh}_3\text{Cl}$  is different from what was observed for Aurbach's APC electrolyte.<sup>10</sup> The difference is ascribed to the different solution constitutions of two electrolytes. During the addition of Cl<sup>-</sup>, coulombic efficiencies for Mg cycling are retained ca. 100% and overpotential stays at ca. 0.29 V. The decrease of Mg cycling current at higher Cl<sup>-</sup> concentration is believed to be ascribed to the change of the chemical equilibrium of the electrolyte solution with Cl<sup>-</sup> as indicated by the <sup>25</sup>Mg NMR spectroscopic studies. There are two possibilities: (a) If the  $[(\mu\text{-Cl})_3\text{Mg}_2(\text{THF})_6]^+$  dimer is the active specie for Mg deposition and stripping, then addition of Cl<sup>-</sup>

can shift the equilibrium to the mononuclear Mg species and lower the concentration of  $[(\mu\text{-Cl})_3\text{Mg}_2(\text{THF})_6]^+$ ; (b) If the solvated  $[\text{MgCl}]^+$  is the active species, the added Cl<sup>-</sup> can complex with  $[\text{MgCl}]^+$  to form solvated MgCl<sub>2</sub> to lower the concentration of the monomeric cation. If MgCl<sub>2</sub> had formed, it would have precipitated out of the solution as it is barely soluble in THF. One explanation is the formed  $[\text{MgCl}_2]$  could complex with the dimer cation to form a soluble trimer cation,  $[\text{Mg}_3(\mu^3\text{-Cl})_2(\mu^2\text{-Cl})_3\text{THF}_6]^{+11}$  (see Scheme 2), consistent with the observed downshift of <sup>25</sup>Mg resonance. It is less likely that  $[\text{MgCl}_2]$  can react with Cl<sup>-</sup> to form  $[\text{MgCl}_3]^{-12}$  and further  $[\text{MgCl}_4]^{2-}$  dianion<sup>10</sup> as these Mg anions would lead to high-field shift of the averaged Mg resonance. We are conducting comprehensive DFT calculations to gain insights to these possible reactions.

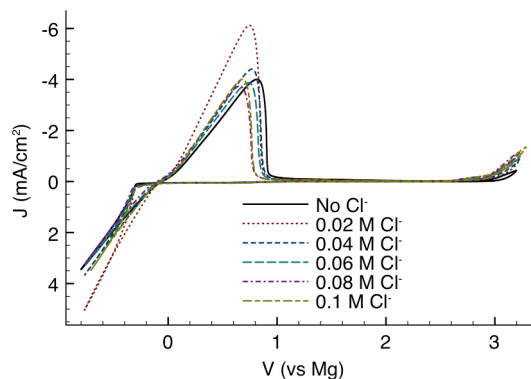
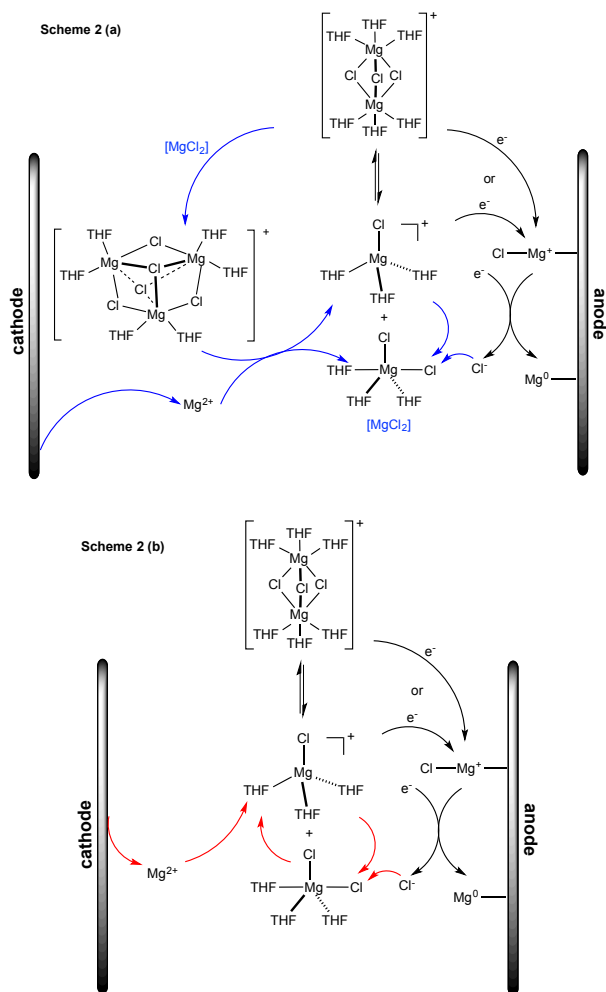


Figure 4. Cyclic voltammograms of  $[(\mu\text{-Cl})_3\text{Mg}_2(\text{THF})_6]\text{AlPh}_3\text{Cl}$  (0.1 M) in the presence of various concentrations of TBACl as indicated. For clearance, cyclic voltammograms with TBACl of 0.01, 0.03, 0.05, 0.07, 0.09 M are given in Figure S5 in the supporting information; conditions: Pt working electrode, Mg reference electrode, glassy carbon counter electrode, 50 mV/s.

In terms of the solution nature of the dimer electrolyte and its reactivity with external Cl<sup>-</sup> described above, comprehensive mechanisms are proposed for Mg<sup>2+</sup> and Cl<sup>-</sup> transports and their involvements with Mg deposition and stripping for the dimer electrolyte in the operation of Mg batteries (scheme 2). The proposed mechanism is an updated version from Aurbach's mechanism<sup>2b</sup> by providing new aspects on Mg electrolyte chemistry. For discussion purpose,  $[\text{MgCl}(\text{THF})_3]^+$  and *cis*-MgCl<sub>2</sub>(THF)<sub>3</sub> will be used as primary equilibrumers with  $[(\mu\text{-Cl})_3\text{Mg}_2(\text{THF})_6]^+$  although they can undergo THF solvation to form  $[\text{MgCl}(\text{THF})_3]^+$  and *trans*-MgCl<sub>2</sub>(THF)<sub>4</sub> (Scheme 1). Either of  $[(\mu\text{-Cl})_3\text{Mg}_2(\text{THF})_6]^+$  or  $[\text{MgCl}(\text{THF})_3]^+$  mono cation on the anodic electrode surface participates the first electron transfer reaction to form a neutral  $[\text{MgCl}]^0$  adsorbed on the electrode. It should be noted that our preliminary DFT calculations suggest the  $[\text{MgCl}]^+$  cation is predominant in solution. Then surface  $[\text{MgCl}]^0$  species undergoes a second electron reduction to result in metallic Mg. It is believed the intermediate of  $[\text{MgCl}]^0$  is the key to the dendrite free deposition of Mg using  $[(\mu\text{-Cl})_3\text{Mg}_2(\text{THF})_6]^+$  electrolytes and its formation is the rate determining step for Mg deposition, providing a kinetic control for overall electron transfer reactions. However, there is no experimental evidence reported for the surface bound species. Such principle can be applied to other anion supported Mg electrolytes.<sup>5b, 13</sup> In the meanwhile, the released Cl<sup>-</sup> will be trapped by  $[\text{MgCl}]^+$  to form  $[\text{MgCl}_2]$  species and subsequently  $[\text{Mg}_3(\mu^3\text{-Cl})_2(\mu^2\text{-Cl})_3\text{THF}_6]^{+}$  (Scheme 2a). Attentively, the solvated Mg<sup>2+</sup> could directly react with  $[\text{MgCl}_2]$  to regenerate  $[\text{MgCl}]^+$  (Scheme 2b).



## Conclusions

We have experimentally identified the long-sought solvated  $[\text{MgCl}]^+$  species in the  $[(\mu\text{-Cl})_3\text{Mg}_2(\text{THF})_6]^+$  electrolyte solution using the SPIN-MS technique, a unique tool to study weakly coordinating complexes. The identified  $[\text{MgCl}]^+$  species confirmed the reaction nature of mono- $\text{Cl}^-$  abstraction of solvated  $\text{MgCl}_2$  with an Al Lewis acid and its role in forming the well known  $[(\mu\text{-Cl})_3\text{Mg}_2(\text{THF})_6]^+$  dimer. We suggest both  $[(\mu\text{-Cl})_3\text{Mg}_2(\text{THF})_6]^+$  and  $[\text{MgCl}(\text{THF})_3]^+$  as mono-cations can be the active species responsible for Mg deposition. Synergetic operation mechanisms of co-existing solvated  $\text{MgCl}_2$  and  $[\text{MgCl}]^+$  was proposed for electrochemical Mg cycling and  $\text{Mg}^{2+}$  and  $\text{Cl}^-$  transports in the operation of Mg batteries. The present fundamental understandings of the coordination chemistry of the Mg-Cl complex electrolytes will inspire synthetic design of next generation of Mg electrolytes for rechargeable Mg batteries.

This work was supported as part of the Joint Center for Energy Storage Research (JCESR), an Energy Innovation Hub funded by the U.S. Department of Energy (DOE), Office of Science, Basic Energy Sciences. Work related to the SPIN source was supported by the NIH National Cancer Institute (IR33CA155252) as well as the General Medical Sciences (GM103491-12) by the Department of Energy Office of Biological and Environmental Research Genome Sciences Program under the Pan-omics project. The Raman and  $^{25}\text{Mg}$  NMR data were collected at William R. Wiley

Environmental Molecular Science Laboratory, a national scientific user facility sponsored by the DOE's Office of Biological and Environmental Research and located at PNNL. PNNL is a multiprogram laboratory operated by Battelle Memorial Institute for DOE.

## Notes and references

<sup>a</sup> Dr. T. Liu, Dr. J. Xiao, Dr. Y. Shao, Dr. J. Liu; Energy Process and Materials Division, Pacific Northwest National Laboratory (PNNL), P.O. Box 999, Richland, WA 99352 (USA); E-mail: Tianbiao.Liu@pnnl.gov; Jun.Liu@pnnl.gov

<sup>b</sup> Dr. J. Cox, Dr. K. Tang, Biological Sciences Division, Pacific Northwest National Laboratory (PNNL), P.O. Box 999, Richland, WA, 99352 (USA)

<sup>c</sup> Dr. D. Hu, Dr. X. Deng, Dr. J. Hu, Dr. M. Y. Hu, William R. Wiley Environmental Molecular Science Laboratory, Pacific Northwest National Laboratory (PNNL), P.O. Box 999, Richland, WA, 99352 (USA)

Electronic Supplementary Information (ESI) available: Information on synthesis and materials, and additional experimental data. See DOI: 10.1039/c000000x/

1 (a) M. Armand and J. M. Tarascon, *Nature*, 2008, **451**, 652; (b) J. Liu, J.-G. Zhang, Z. Yang, J. P. Lemmon, C. Imhoff, G. L. Graff, L. Li, J. Hu, C. Wang, J. Xiao, G. Xia, V. V. Viswanathan, S. Baskaran, V. Sprenkle, X. Li, Y. Shao and B. Schwenzer, *Adv. Funct. Mater.*, 2013, **23**, 929; (c) Z. Yang, J. Zhang, M. C. W. Kintner-Meyer, X. Lu, D. Choi, J. P. Lemmon and J. Liu, *Chem. Rev.*, 2011, **111**, 3577; (d) J. B. Goodenough and K.-S. Park, *J. Am. Chem. Soc.*, 2013, **135**, 1167.

2 (a) J. Muldoon, C. B. Bucur, A. G. Oliver, T. Sugimoto, M. Matsui, H. S. Kim, G. D. Allred, J. Zajicek and Y. Kotani, *Energy Environ. Sci.*, 2012, **5**, 5941; (b) H. D. Yoo, I. Shterenberg, Y. Gofar, G. Gershinsky, N. Pour and D. Aurbach, *Energy Environ. Sci.*, 2013, **6**, 2265; (c) H. Kim, G. Jeong, Y.-U. Kim, J.-H. Kim, C.-M. Park and H.-J. Sohn, *Chem. Soc. Rev.*, 2013.

3 T. D. Gregory, R. J. Hoffman and R. C. Winterton, *J. Electrochem. Soc.*, 1990, **137**, 775.

4 (a) D. Aurbach, Z. Lu, A. Schechter, Y. Gofar, H. Gizbar, R. Turgeman, Y. Cohen, M. Moshkovich and E. Levi, *Nature*, 2000, **407**, 724; (b) N. Pour, Y. Gofar, D. T. Major and D. Aurbach, *J. Am. Chem. Soc.*, 2011, **133**, 6270.

5 (a) Y. Guo, F. Zhang, J. Yang, F. Wang, Y. NuLi and S. Hirano, *Energy Environ. Sci.*, 2012, **5**, 9100; (b) R. Mohtadi, M. Matsui, T. S. Arthur and S.-J. Hwang, *Angew. Chem. Int. Ed.*, 2012, **51**, 9780; (c) H. S. Kim, T. S. Arthur, G. D. Allred, J. Zajicek, J. G. Newman, A. E. Rodnyansky, A. G. Oliver, W. C. Boggess and J. Muldoon, *Nat. Commun.*, 2011, **2**, 2; (d) L. V. T. Xu, P. Saha, M. K. Datta, M. L. Gordin, A. Manivannan, P. N. Kumta and D. Wang, *J. Electrochem. Soc.*, 2013, **160**, A351; (e) D. Lv, D. Tang, Y. Duan, M. L. Gordin, F. Dai, P. Zhu, J. Song, A. Manivannan and D. Wang, *J. Mater. Chem. A.*, 2014, **2**, 15488.

6 T. Liu, Y. Shao, G. Li, M. Gu, J. Hu, S. Xu, Z. Nie, X. Chen, C. Wang and J. Liu, *J. Mater. Chem. A.*, 2014, **2**, 3430.

7 S. Sakamoto, T. Imamoto and K. Yamaguchi, *Org. Lett.*, 2001, **3**, 1793.

8 (a) J. S. Page, K. Tang, R. T. Kelly and R. D. Smith, *Anal. Chem.*, 2008, **80**, 1800; (b) I. Marginean, J. S. Page, A. V. Tolmachev, K. Tang and R. D. Smith, *Anal. Chem.*, 2010, **82**, 9344; (c) I. Marginean, S. R. Kronewitter, R. J. Moore, G. W. Slys, M. E. Monroe, G. Anderson, K. Tang and R. D. Smith, *Anal. Chem.*, 2012, **84**, 9208.

9 L. F. Wan and D. Prendergast, *J. Am. Chem. Soc.*, 2014, **136**, 14456.

10 Y. Gofar, O. Chusid, H. Gizbar, Y. Viestfrid, H. E. Gottlieb, V. Marks and D. Aurbach, *Electrochem. Solid-State Lett.*, 2006, **9**, A257.

11 C. J. Barile, E. C. Barile, K. R. Zavadil, R. G. Nuzzo and A. A. Gewirth, *The Journal of Physical Chemistry C*, 2014.

12 C. Liao, B. Guo, D.-e. Jiang, R. Custelcean, S. M. Mahurin, X.-G. Sun and S. Dai, *J. Mater. Chem. A.*, 2014, **2**, 581.

13 Y. Shao, T. Liu, G. Li, M. Gu, Z. Nie, M. Engelhard, J. Xiao, D. Lv, C. Wang, J.-G. Zhang and J. Liu, *Sci. Rep.*, 2013, **3**.